ACS APPLIED MATERIALS & INTERFACES

Research Article

www.acsami.org

# Uniform Small Graphene Oxide as an Efficient Cellular Nanocarrier for Immunostimulatory CpG Oligonucleotides

Jinli Sun,[†,∥] Jie Chao,[‡,∥] Jing Huang,[§,∥] Min Yin,[‡] Huan Zhang,[‡] Cheng Peng,[‡] Zengtao Zhong,*[,†] and Nan Chen*[,‡]

[†]College of Life Sciences, Nanjing Agriculture University, Nanjing 210095, China

[‡]Division of Physical Biology and Bioimaging Center, Shanghai Synchrotron Radiation Facility, CAS Key Laboratory of Interfacial Physics and Technology, Shanghai Institute of Applied Physics, Chinese Academy of Sciences, Shanghai 201800, China

[§]Department of Neurology, Shanghai Tenth People's Hospital, School of Medicine, Shanghai 200072, China

Supporting Information

**ABSTRACT:** Graphene oxide (GO) has attracted more and more attention as a promising nanomaterial in biomedical research and applications. In this study, we explore the ability of GO as nanocarrier for synthetic DNA strands. Immunostimulatory CpG oligodeoxynucleotides (ODNs) are attached to Poly-L-Lysine (PLL) functionalized, polydisperse GO, or uniform small GO (sGO) nanosheets. Both types of GO-CpG ODN nanoconjugates can be delivered into murine Raw264.7 macrophages and possess immunostimulatory activity, while sGO-CpG appears to be a more efficient stimulator. In addition, sGO-CpG nanosheets exhibit higher cellular uptake but better biocompatibility compared to the larger GO-CpG counterpart. Furthermore, PLL functionalized sGO-CpG has higher immunostimulatory activity than azide functionalized sGO-CpG. Together, our studies provide evidence that sGO can be utilized as an ideal intracellular nanocarrier for synthetic single-stranded DNA, and sGO-PLL-CpG conjugates may serve as a potential proinflammatory therapeutic tool.

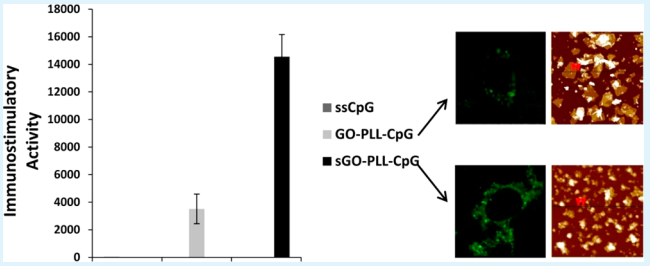


**KEYWORDS:** *graphene oxide, uniform small, CpG ODN, nanocarrier, immunostimulatory activity*

## INTRODUCTION

Synthetic oligonucleotides, such as antisense DNA, aptamers, and small interfering RNAs (siRNAs), are highly attractive candidates for clinical therapeutic applications.[1−3] However, naked oligodeoxynucleotides (ODNs) cannot actively pass through the cell membrane and are prone to being degraded by nucleases before finding their targets. It is highly demanding to build simple and efficient delivery strategies for ODNs, which can simultaneously address multiple challenges including the efficiency of cellular uptake, protection from nuclease degradation, conservation of bioactivities, and potential cellular toxicities of delivery vehicles.[4−6] The rapid progress of nanobiotechnology has provided unprecedented opportunities to develop biocompatible, low-toxicity, and highly efficient approaches for exogenous ODN administration in target organs or cells.[7−11]

Graphene oxide (GO), a two-dimensional carbon nanosheet, is a heavily oxidized graphene derivative. Due to its large surface area, high stability in aqueous dispersion, and low cyto-toxicity, GO has been widely explored for biological and biomedical applications,[12−15] including bioimaging,[16,17] biosensors,[17−19] and drug and ODN delivery.[20−23] GO sheets are conventionally prepared by a random "top-down" chemical exfoliation from graphite powder,[24] which results in polydisperse lateral sizes ranging from tens of nanometers to a few micrometers and greatly limits its potential applications.[25] Therefore, several approaches have been developed to synthesize GO sheets with uniform small size, such as density gradient ultracentrifugal rate separation[26] and pH-assisted selective sedimentation.[27] Recently, our group has developed a high yield and low-cost method to produce uniform ultrasmall GO (sGO) nanosheets via several rounds of oxidation.[28] These nanosheets have a lateral size of less than 50 nm and exhibit better biocompatibility and higher cellular uptake efficiency compared to polydisperse GO.

Unmethylated cytosine−guanine (CpG) dinucleotide motifs, which occur frequently in viral and bacterial genomes but rarely in mammalian genomes, can be recognized by endosome localized Toll-like receptor 9 (TLR9) of host cells and induce the expression of proflammatory cytokines via the NFκB pathway and the MAPK pathway.[29−33] Synthetic CpG ODNs show similar immunostimulatory activity and are widely used as a therapeutic tool for various diseases including infection, allergies, and cancer.[34−38] Several studies including ours have explored new approaches based on nanotechnology to enhance cellular uptake and immunostimulatory effects of CpG

Received: March 1, 2014
Accepted: April 8, 2014
Published: April 8, 2014





dx.doi.org/10.1021/am5012595 | ACS Appl. Mater. Interfaces 2014, 6, 7926−7932

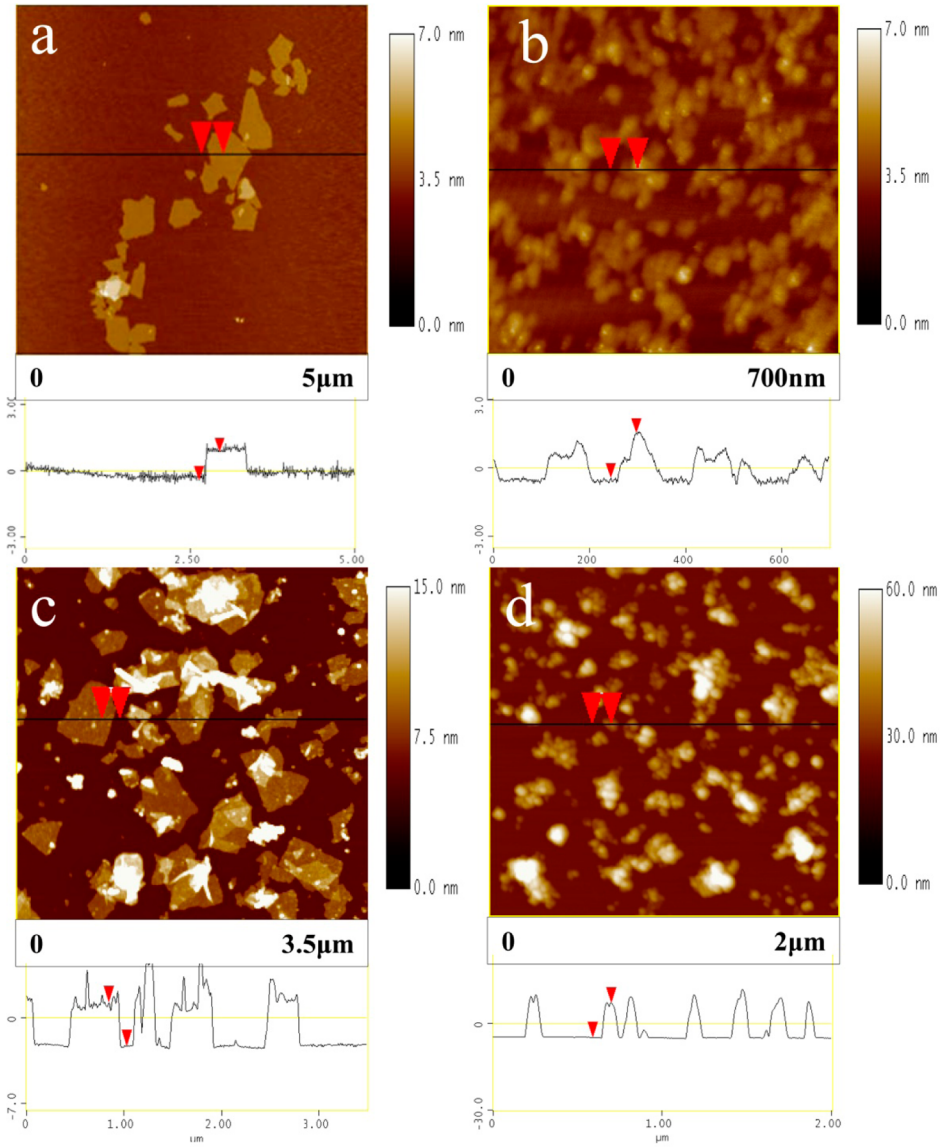


**Figure 1.** Characterizations of GO and GO-PLL. AFM images of GO (a), sGO (b), GO-PLL (c), and sGO-PLL (d).

ODNs.[39−43] Various DNA nano-assemblies, nanoparticles, and nanotubes have been utilized as carriers for CpG ODNs.[44−47] While these methods have significantly improved the applicability of CpG ODNs in biological studies and even clinical trials, safer, simpler, and low-cost strategies for the administration of CpG ODNs are still in demand.

In this study, we aimed to explore the ability of GO as a cellular nanocarrier for immunostimulatory CpG ODNs, using either polydisperse GO or uniform sGO. These two types of CpG nanoconjugates were compared in their cytotoxicity, cellular uptake efficiency, and immunostimulatory activities. In addition, we tested the possibility of PLL and azide as ideal crosslinkers between GO and CpG ODNs and compared their effects on immunostimulatory activities of CpG nanoconjugates. Our results revealed PLL functionalized sGO as biocompatible and a highly efficient delivery vehicle for CpG ODNs.

## RESULTS AND DISCUSSION

**Characterization of CpG Nanoconjugates.** Polydisperse GO was synthesized according to a modified Hummers' method.[24] Repeated oxidation was then performed to obtain uniformed sGO nanosheets. As shown in Figure S1, the solution of sGO had lighter color compared to GO, indicating reduced light absorption during oxidation. Atomic force microscopy (AFM) images of two types of GO nanosheets were showed in Figure 1a and b. The thicknesses of GO and sGO were quite similar, ranging from about 1.1 nm to 1.4 nm. However, their lateral sizes were dramatically different. The lateral size of polydisperse GO ranged from hundreds of nanometers to several micrometers, while the lateral size of sGO nanosheets was quite uniform and was less than 50 nm. Two types of GO nanosheets were subsequently functionalized with PLL. The lateral size of PLL-conjugated GO or sGO was not changed by this covalent modification, while the thicknesses of both GO nanosheets were significantly increased. The thickness of polydisperse GO was about 3.6 nm, indicating the coverage of PLL on the nanosheets. Of note, the thickness of sGO was about 10 nm, suggesting the formation of multilayers of the sGO-PLL nanocomplex (Figure 1c and d). Both GO-PLL and sGO-PLL solution turned darker in color (Figure S1), which also confirmed the covalent modification.


dx.doi.org/10.1021/am5012595 | ACS Appl. Mater. Interfaces 2014, 6, 7926−7932

PLL functionalization provides plenty of amino groups for electrostatic interaction with negatively charged CpG ODNs. The efficiency of CpG ODNs absorption was compared between GO-PLL and sGO-PLL. As shown in Table S2, both GO-PLL and sGO-PLL can absorb more than 90% of total CpG ODN in solution as determined by the reduction of UV absorption. With an increased amount of GO-PLL/sGO-PLL in the mixture, absorption of CpG ODNs was slightly increased.

**Cytotoxicity of CpG Nanoconjugates.** Ideal delivery vehicles for CpG ODNs must present good biocompatibility. Therefore, we examined the cytotoxicity of GO-PLL, sGO-PLL, and corresponding CpG conjugates at various concentrations (6.25-50 ug/mL) in RAW264.7 cells. At 6.25 ug/mL, GO-PLL and sGO-PLL slightly reduced cell viability, while neither GO-PLL-CpG nor sGO-PLL-CpG showed noticeable cytotoxicity. The effect of GO-PLL-CpG or sGO-PLL-CpG on cell viability could be observed at higher concentrations, with the latter showing less toxicity. At the highest concentration tested (50 ug/mL), GO-PLL-CpG and sGO-PLL-CpG reduced the viability of RAW264.7 cells by 28% and 15%, respectively (Figure 2). Interestingly, sGO-PLL-CpG showed slightly but consistently less toxicity than sGO-PLL at various concentrations, suggesting that CpG ODNs could enhance the biocompatibility of its carrier.

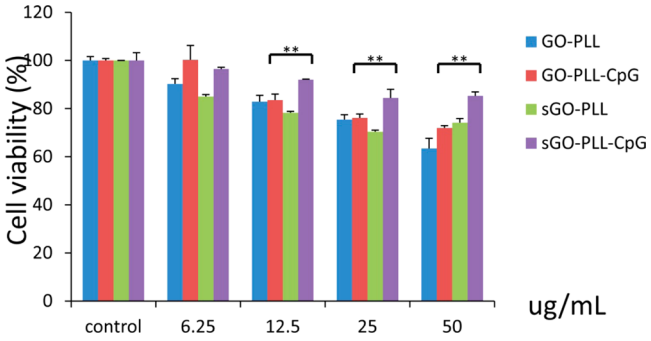


**Figure 2.** Cytotoxicity of GO-PLL, sGO-PLL, and corresponding CpG conjugates. Raw 264.7 cells were incubated with indicated materials for 24 h, and cell viability was determined (t-test: **p < 0.01).

**Immunostimulatory Activity of CpG Nanoconjugates.** To test whether these conjugations affect the bioactivity of CpG ODNs, we incubated these CpG nanoconjugates with RAW264.7 cells and examined their immunostimulatory activities by measuring levels of secreted proflammatory cytokines in the medium. While GO-PLL or sGO-PLL alone had no immunostimulatory activity, both GO-PLL-CpG and sGO-PLL-CpG stimulated secretion of TNF-$\alpha$ and IL-6. At a concentration of 50 ug/mL, the immunostimulatory activity of sGO-PLL-CpG was significantly higher than that of GO-PLL-CpG and comparable or higher than that of S-CpG, a nuclease-resistant CpG derivative (Figure 3a and b). We also measured immunostimulatory effects of GO-PLL-CpG and sGO-PLL-CpG at various concentrations. Both types of CpG nanoconjugates stimulated cytokine secretion in a concentration dependent manner (Figure 4). These results suggested that both GO-PLL and sGO-PLL could deliver functional CpG ODNs into RAW264.7 cells and induce immune responses, with sGO-PLL-CpG being a better stimulator.

**Cellular Internalization of CpG Nanoconjugates.** Our previous results showed that uniform sGO had a higher cellular uptake efficiency than polydisperse GO. It is likely that sGO-PLL-CpG was also internalized in RAW264.7 cells more efficiently than GO-PLL-CpG and induced higher immunostimulatory effects. To test this possibility, we assembled Cy3-labeled CpG ODNs on GO-PLL or sGO-PLL and monitored their levels of cellular internalization in RAW264.7 cells. As a control, no fluorescent signal was observed in cells incubated with free ssCpG-Cy3 ODNs (Figure 5a). Conjugation of CpG-Cy3 to either GO-PLL or sGO-PLL resulted in clear fluorescent signal in the cytoplasm. In addition, the signal from sGO-PLL-CpG-Cy3 treated cells was much stronger than that from GO-PLL-CpG-Cy3 treated cells (Figure 5b and c). Therefore, sGO-PLL is a better nanocarrier than GO-PLL in the cellular delivery of CpG ODNs.

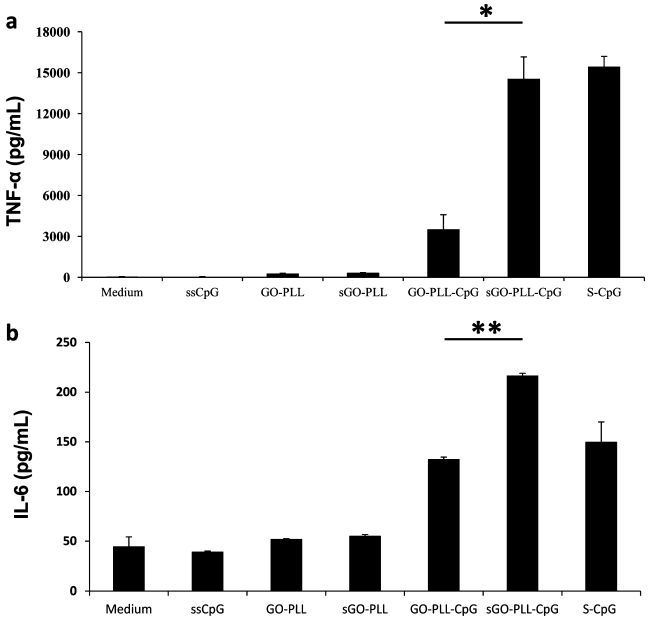


**Figure 3.** Immunostimulatory activity of GO-PLL, sGO-PLL, and corresponding CpG conjugates. RAW264.7 cells were treated with the indicated materials. Secretion of TNF-$\alpha$ (a) and IL-6 (b) was measured 8 and 24 h later, respectively. Concentration of CpG-ODNs was 400 nM. GO-PLL or sGO-PLL (50$\mu$g/mL) was used as control (t-test: **p < 0.01, *p < 0.05).

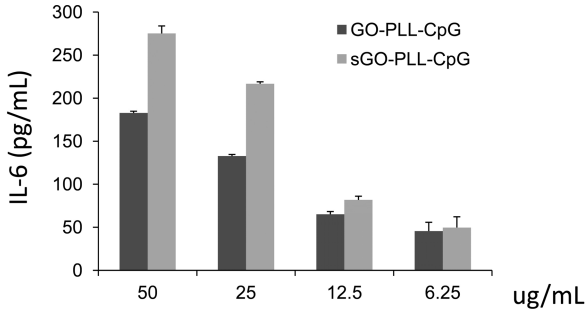


**Figure 4.** CpG nanoconjugates stimulate secretion of cytokines in a concentration dependent manner. RAW264.7 cells were treated with indicated materials, and secretion of IL-6 was measured.

**Effects of Crosslinkers on Immunostimulatory Activity of CpG Nanoconjugates.** The crosslinker that conjugates CpG ODNs to GO can also have a potential effect on the bioactivity of CpG ODNs, presumably by directly or indirectly affecting interactions between CpG ODNs and TLR9. We have previously shown that azide functionalized GO can be also

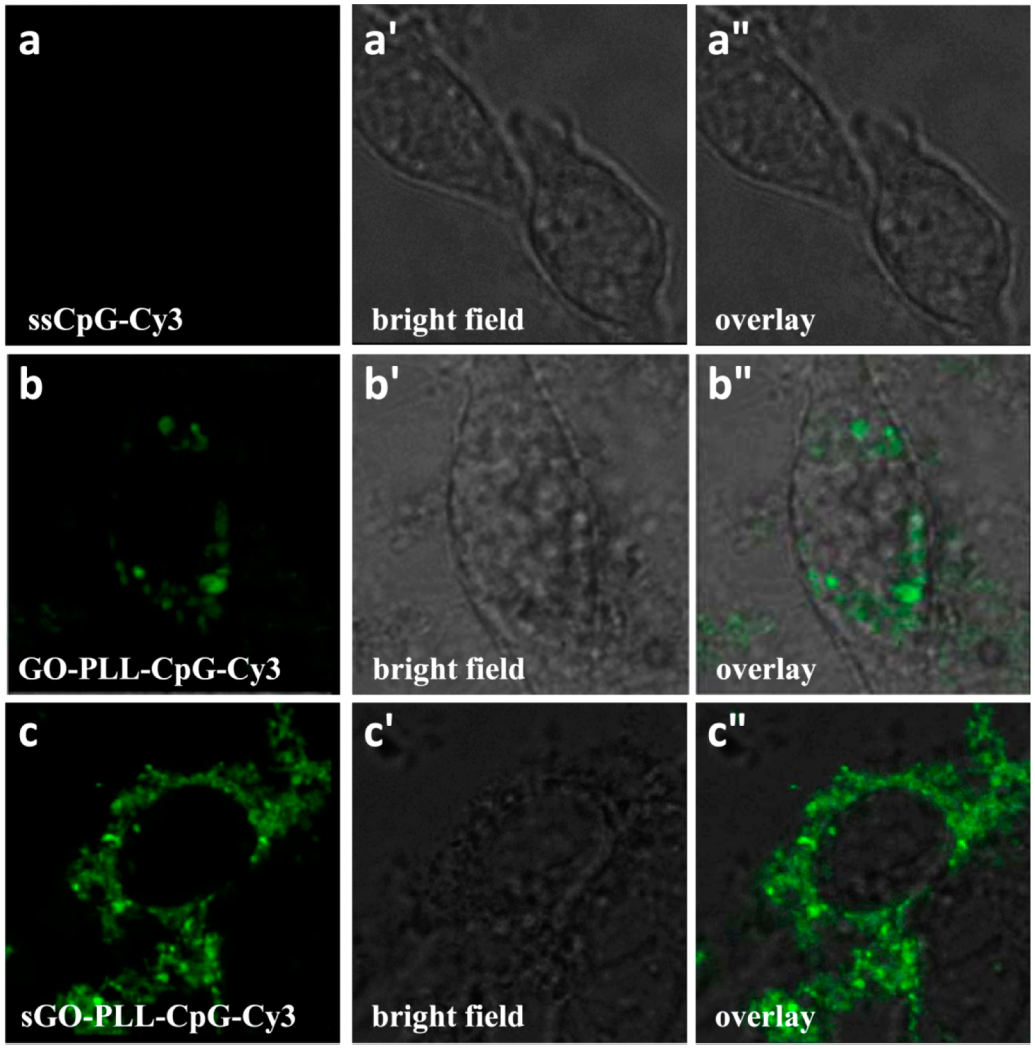


**Figure 5.** Cellular internalization of CpG nanoconjugates. RAW264.7 cells were treated with ssCpG-Cy3 (a), GO-PLL-CpG-Cy3 (b), or sGO-PLL-CpG-Cy3 (c) for 4 h. Relative cellular uptake and localization of CpG were shown by Confocal images.

conjugated to DNA strands.[48] Thus, we tested whether GO-azide (GO-Az) could function as a delivery vehicle for CpG ODNs and compared effects of azide and PLL on the immunostimulatory activity of CpG nanoconjugates. Both GO-Az-CpG and sGO-Az-CpG stimulated secretion of cytokines from RAW264.7 cells. Consistent with the above results, sGO-Az-CpG had higher immunostimulatory effects than GO-Az-CpG (Figure 6). While GO-Az-CpG and GO-PLL-CpG showed comparable immunostimulatory activities, sGO-Az-CpG showed significantly lower activity than sGO-PLL-CpG, suggesting that azide might have an adverse effect on the bioactivity of CpG ODNs when the celluar uptake efficiency was high (Figure 7). As a result, sGO-PLL is a better delivery vehicle for CpG ODN than sGO-Az. To look for underlying reasons, we noticed that GO-Az and sGO-Az already showed some immunostimulatory activities (Figure 6), suggesting that they might affect TLR9 either specifically or non-specifically and might interfere with interactions between CpG ODNs and TLR9.

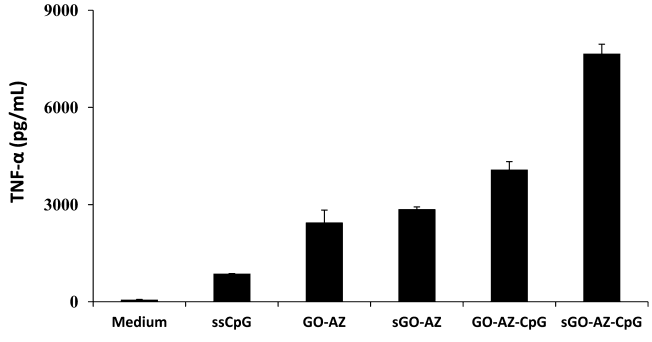


**Figure 6.** Azide modified CpG nanoconjugates stimulate secretion of cytokines. RAW264.7 cells were treated with indicated materials for 8 h, and secreted TNF-$\alpha$ was measured. The concentration of CpG-ODN was 400 nM. An equal amount of GO-Az or sGO-Az (50$\mu$g/mL) was used as control.

## CONCLUSIONS

GO has a great potential in nanotechnology and biomedicine. Here, we showed that GO could serve as cellular nanocarrier for synthetic DNA strands. Compared to polydisperse GO-CpG conjugates, uniform ultrasmall GO-CpG conjugates exhibited better biocompatibility, higher cellular uptake efficiency, and higher immunostimulatory activity. In addition, our results suggested that crosslinkers between GO nanosheets and CpG ODNs could have an effect on the bioactivity of

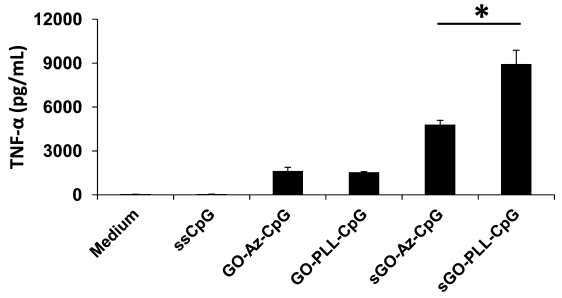


**Figure 7.** Comparison of immunostimulatory activity between azide and PLL modified GO-CpG conjugates. RAW264.7 cells were treated with indicated materials for 8 h, and secreted TNF-$\alpha$ was measured. The concentration of CpG-ODNs was 400 nM (t-test: **p < 0.01, *p < 0.05).

delivered DNA strands. Ideal crosslinkers that can facilitate interactions between synthetic ODNs and their targets should be explored in the future.

## EXPERIMENTAL SECTION

**Materials.** Graphite, $NaBH_4$, and KOH were obtained from Sinopharm Chemical Reagent Co. 2-Chloroethyl isocyanate, sodium azide, poly-L-lysine hydrobromide (PLL, $M_w$ = 30 000−70 000), avidin-peroxidase, thiazolyl blue tetrazolium bromide (MTT), and sodium dodecyl sulfate (SDS) were purchased from Sigma-Aldrich (USA). Purified anti-mouse TNF-$\alpha$, biotin conjugated anti-mouse TNF-$\alpha$ cocktail, recombination mouse TNF-$\alpha$, anti-mouse IL-6, biotin anti-mouse IL-6, and recombinant mouse IL-6 were purchased from eBioscience. K-blue TMB substrate was purchased from Neogen Co. The alkynyl functionalized CpG oligodeoxynucleotides (ODNs) were synthesized and purified by TaKaRa Inc.; CpG ODNs and fluorophore-labeled CpG ODNs were synthesized and purified by Invitrogen, and the sequences are shown in Table S1. The mouse leukemic monocyte macrophage RAW264.7 cell line was purchased from Cell Bank of Chinese Academy of Sciences (Shanghai).

**Instruments.** Atomic force microscopy (AFM) images were recorded using a Nanoscope IIIa apparatus (Digital Instruments, USA) equipped with a J Scanner. Cellular uptake images of a fluorophore-labeled CpG ODN were obtained using a Laser confocal microscope (Leica TCS SP5).

**Preparation of Functionalized Graphene Oxide Sheets and Corresponding CpG Nanoconjugates.** GO nanosheets and uniform ultrasmall GO (sGO) nanosheets were prepared as previously described.[28] PLL or azide modification of GO and sGO was performed with the method described in previous studies.[48,49] Negatively charged CpG ODNs were surface immobilized onto positively charged graphene oxide-PLL via electrostatic interactions. The diluted graphene oxide-PLL solution (50$\mu$L, 0.5 mg/mL) was mixed with a CpG ODN solution (50$\mu$L, 50ug/mL) at a mass ratio of 20:1. Samples were ultrasonicated for 30 min and stirred for 2 h at room temperature to obtain the final conjugates. Graphene oxide-Az-CpG was prepared through the "click" reaction as previously described.

**Atomic Force Microscopy (AFM).** The size and thickness of GO-PLL and sGO-PLL were measured by AFM. Aqueous solutions of GO-PLL and sGO-PLL for each experimental condition were prepared at a concentration of 0.25 mg/mL and spin-coated on silicon dioxide surfaces measuring about 12 $mm^2$. $SiO_2$ was cleaned in argon plasma for at least 10 min prior to spin coating. Spin coating was performed for 5.5 min at 3500 rpm with 75 $\mu$L of sample solution (enough to completely wet the cleaned $SiO_2$ surface). Imaging was performed using a Nanoscope IIIa apparatus (Digital Instruments, USA) equipped with a J Scanner.

**Cytotoxicity Assays.** RAW264.7 cells were cultured in 96-well plates overnight to reach ~80% confluency. Fresh media containing graphene-PLL or graphene-PLL-CpG at indicated concentrations were incubated with cells for 24 h. Fifty microliters of 5 mg/mL thiazolyl blue tetrazolium bromide (MTT, Sigma-Aldrich, USA) solution was then added to each well, followed by 4 h of incubation at 37 °C. Next, cells were lysed with a 10% acid SDS solution (pH 2−3). After centrifugation, the absorbance of the supernatant was measured at 570 nm with a microplate reader (Bio-Rad 680, USA).

**Characterization of Cellular Uptake of Nanoconjugates in RAW264.7 Cells.** Cy3-labeled CpG ODN strands were used for preparation of fluorescence labeled PLL-graphene nanosheets. RAW264.7 cells were cultured on glass coverslips at 37 °C. Twenty-four hours later, cells were washed with PBS, exposed to a fresh culture medium containing graphene-PLL-CpG-Cy3 or naked CpG-Cy3 for 4 h, and washed three times with PBS. Cells were then fixed with 3% paraformaldehyde/sucrose. The coverslips were mounted on glass slides. Cellular uptake of CpG-Cy3 ODNs was measured with a laser confocal microscope (Leica TCS SP5).

**Measurement of Cytokine Secretion from RAW264.7 Cells.** RAW264.7 cells were cultured in 24-well plates at a density of 2.5 × $10^5$ cells/well. After 24 h, cells were washed with 0.5 mL of PBS before treatment with various GO nanoconjugates. The medium was collected 8 h later for measurement of TNF-$\alpha$ secretions, or 24 h later for measurement of IL-6 secretions. The levels of secreted TNF-$\alpha$ and IL-6 were measured with a sandwich ELISA method using protocols recommended by the manufacturer.

## ASSOCIATED CONTENT

### Supporting Information

More characterizations of the materials and sequences of ODNs used in this work are included. This material is available free of charge via the Internet at http://pubs.acs.org.

## AUTHOR INFORMATION

### Corresponding Authors

*E-mail: ztzhong@njau.edu.cn.
*E-mail: chennan@sinap.ac.cn.

### Author Contributions

‖These authors contributed equally to this work.

### Notes

The authors declare no competing financial interest.

## ACKNOWLEDGMENTS

This work was financially supported by National Natural Science foundation of China (31100716, U1332119, 51102272), CAS (KJCX2-EWN03), the Fundamental Research Funds for the Central Universities (KYZ201317), and Shanghai Pujiang Program (12PJ1410600).

## REFERENCES

(1) Dorsett, Y.; Tuschl, T. siRNAs: Applications in Functional Genomics and Potential as Therapeutics. *Nat. Rev. Drug Discovery* **2004**, *3*, 318−329.
(2) Agrawal, S.; Zhao, Q. Y. Antisense Therapeutics. *Curr. Opin. Chem. Biol.* **1998**, *2*, 519−528.
(3) Lebedeva, I.; Stein, C. A. Antisense Oligonucleotides: Promise and Reality. *Annu. Rev. Pharmacol. Toxicol.* **2001**, *41*, 403−19.
(4) Seferos, D. S.; Prigodich, A. E.; Giljohann, D. A.; Patel, P. C.; Mirkin, C. A. Polyvalent DNA Nanoparticle Conjugates Stabilize Nucleic Acids. *Nano Lett.* **2009**, *9*, 308−11.
(5) Gopalakrishnan, B.; Wolff, J. siRNA and DNA Transfer to Cultured Cells. *Methods Mol. Biol.* **2009**, *480*, 31−52.
(6) Mintzer, M. A.; Simanek, E. E. Nonviral Vectors for Gene Delivery. *Chem. Rev.* **2009**, *109*, 259−302.
(7) Dhar, S.; Daniel, W. L.; Giljohann, D. A.; Mirkin, C. A.; Lippard, S. J. Polyvalent Oligonucleotide Gold Nanoparticle Conjugates as Delivery Vehicles for Platinum(IV) Warheads. *J. Am. Chem. Soc.* **2009**, *131*, 14652−14653.

(8) Giljohann, D. A.; Seferos, D. S.; Prigodich, A. E.; Patel, P. C.; Mirkin, C. A. Gene Regulation with Polyvalent siRNA-Nanoparticle Conjugates. *J. Am. Chem. Soc.* **2009**, *131*, 2072−3.
(9) Viktoriya, S.; Matthias, E. Inorganic Nanoparticles as Carriers of Nucleic Acids into Cells. *Angew. Chem., Int. Ed.* **2008**, *47*, 1382−1395.
(10) Lee, J. H.; Yigit, M. V.; Mazumdar, D.; Lu, Y. Molecular Diagnostic and Drug Delivery Agents Based on Aptamer-Nanomaterial Conjugates. *Adv. Drug Delivery Rev.* **2010**, *62*, 592−605.
(11) Li, J.; Fan, C.; Pei, H.; Shi, J.; Huang, Q. Smart Drug Delivery Nanocarriers with Self-assembled DNA Nanostructures. *Adv. Mater.* **2013**, *25*, 4386−96.
(12) Zhang, X.; Yin, J.; Peng, C.; Hu, W.; Zhu, Z.; Li, W.; Fan, C.; Huang, Q. Distribution and Biocompatibility Studies of Graphene Oxide in Mice after Intravenous Administration. *Carbon.* **2011**, *49*, 986−995.
(13) Shen, H.; Zhang, L. M.; Liu, M.; Zhang, Z. J. Biomedical Applications of Graphene. *Theranostics* **2012**, *2*, 283−294.
(14) Robinson, J. T.; Tabakman, S. M.; Liang, Y.; Wang, H.; Casalongue, H. S.; Vinh, D.; Dai, H. Ultrasmall Reduced Graphene Oxide with High Near-Infrared Absorbance for Photothermal Therapy. *J. Am. Chem. Soc.* **2011**, *133*, 6825−31.
(15) Tang, J.; Chen, Q.; Xu, L.; Zhang, S.; Feng, L.; Cheng, L.; Xu, H.; Liu, Z.; Peng, R. Graphene Oxide-silver Nanocomposite as a Highly Effective Antibacterial Agent with Species-specific Aechanisms. *ACS Appl. Mater. Interfaces* **2013**, *5*, 3867−3874.
(16) Peng, C.; Hu, W.; Zhou, Y.; Fan, C.; Huang, Q. Intracellular Imaging with a Graphene-Based Fluorescent Probe. *Small* **2010**, *6*, 1686−1692.
(17) Sun, X. M.; Liu, Z.; Welsher, K.; Robinson, J. T.; Goodwin, A.; Zaric, S.; Dai, H. J. Nano-Graphene Oxide for Cellular Imaging and Drug Delivery. *Nano Res.* **2008**, *1*, 203−212.
(18) Li, F.; Huang, Y.; Yang, Q.; Zhong, Z.; Li, D.; Wang, L.; Song, S.; Fan, C. A Graphene-Enhanced Molecular Beacon for Homogeneous DNA Detection. *Nanoscale* **2010**, *2*, 1021−6.
(19) Wen, Y.; Peng, C.; Li, D.; Zhuo, L.; He, S.; Wang, L.; Huang, Q.; Xu, Q. H.; Fan, C. Metal Ion-Modulated Graphene-DNAzyme Interactions: Design of a Nanoprobe for Fluorescent Detection of Lead(II) Ions with High Sensitivity, Selectivity and Tunable Dynamic Range. *Chem. Commum.* **2011**, *47*, 6278−6280.
(20) Liu, Z.; Robinson, J. T.; Sun, X.; Dai, H. PEGylated Nanographene Oxide for Delivery of Water-Insoluble Cancer Drugs. *J. Am. Chem. Soc.* **2008**, *130*, 10876−7.
(21) Zhang, L. M.; Xia, J. G.; Zhao, Q. H.; Liu, L. W.; Zhang, Z. J. Functional Graphene Oxide as a Nanocarrier for Controlled Loading and Targeted Delivery of Mixed Anticancer Drugs. *Small* **2010**, *6*, 537−544.
(22) Tan, X.; Feng, L.; Zhang, J.; Yang, K.; Zhang, S.; Liu, Z.; Peng, R. Functionalization of Graphene Oxide Generates a Unique Interface for Selective Serum Protein Interactions. *ACS Appl. Mater. Interfaces* **2013**, *5*, 1370−1377.
(23) Singh, S. K.; Singh, M. K.; Kulkarni, P. P.; Sonkar, V. K.; Gracio, J. J.; Dash, D. Amine-Modified Graphene: Thrombo-Protective Safer Alternative to Graphene Oxide for Biomedical Applications. *ACS Nano* **2012**, *6*, 2731−40.
(24) Hummers, W. S.; Offeman, R. E. Preparation of Graphitic Oxide. *J. Am. Chem. Soc.* **1958**, *80*, 1339−1339.
(25) Chung, C.; Kim, Y. K.; Shin, D.; Ryoo, S. R.; Hong, B. H.; Min, D. H. Biomedical Applications of Graphene and Graphene Oxide. *Acc. Chem. Res.* **2013**, *46*, 2211−24.
(26) Sun, X. M.; Luo, D. C.; Liu, J. F.; Evans, D. G. Monodisperse Chemically Modified Graphene Obtained by Density Gradient Ultracentrifugal Rate Separation. *ACS Nano* **2010**, *4*, 3381−3389.
(27) Wang, X.; Bai, H.; Shi, G. Size Fractionation of Graphene Oxide Sheets by pH-Assisted Selective Sedimentation. *J. Am. Chem. Soc.* **2011**, *133*, 6338−42.
(28) Zhang, H.; Peng, C.; Yang, J.; Lv, M.; Liu, R.; He, D.; Fan, C.; Huang, Q. Uniform Ultrasmall Graphene Oxide Nanosheets with Low Cytotoxicity and High Cellular Uptake. *ACS Appl. Mater. Interfaces* **2013**, *5*, 1761−7.
(29) Krieg, A. M. CpG Motifs in Bacterial DNA and Their Immune Effects. *Annu. Rev. Immunol.* **2002**, *20*, 709−60.
(30) Krieg, A. M.; Yi, A. K.; Matson, S.; Waldschmidt, T. J.; Bishop, G. A.; Teasdale, R.; Koretzky, G. A.; Klinman, D. M. CpG Motifs in Bacterial DNA Trigger Direct B-cell Activation. *Nature* **1995**, *374*, 546−9.
(31) Agrawal, S.; Kandimalla, E. R. Medicinal Chemistry and Therapeutic Potential of CpG DNA. *Trends. Mol. Med.* **2002**, *8*, 114−121.
(32) Hemmi, H.; Kaisho, T.; Takeda, K.; Akira, S. The Roles of Toll-like Receptor 9, MyD88, and DNA-Dependent Protein Kinase Catalytic Subunit in the Effects of Two Distinct CpG DNAs on Dendritic Cell Subsets. *J. Immunol.* **2003**, *170*, 3059−64.
(33) Krieg, A. M. Therapeutic Potential of Toll-like Receptor 9 Activation. *Nat. Rev. Drug Discovery* **2006**, *5*, 471−84.
(34) Wu, F.; Yuan, X. Y.; Li, J.; Chen, Y. H. The Co-Administration of CpG-ODN Influenced Protective Activity of Influenza M2e Vaccine. *Vaccine* **2009**, *27*, 4320−4.
(35) Kim, H. A.; Ko, H. M.; Ju, H. W.; Kim, K. J.; Roh, S. G.; Lee, H. K.; Im, S. Y. CpG-ODN-Based Immunotherapy is Effective in Controlling the Growth of Metastasized Tumor Cells. *Cancer Lett.* **2009**, *274*, 160−4.
(36) Klinman, D. M. Immunotherapeutic Uses of CpG Oligodeoxynucleotides. *Nat. Rev. Immunol.* **2004**, *4*, 248−257.
(37) Olbert, P. J.; Schrader, A. J.; Simon, C.; Dalpke, A.; Barth, P.; Hofmann, R.; Hegele, A. In Vitro and in Vivo Effects of CpG-Oligodeoxynucleotides (CpG-ODN) on Murine Transitional Cell Carcinoma and on the Native Murine Urinary Bladder Wall. *Anticancer Res.* **2009**, *29*, 2067−76.
(38) Beaudette, T. T.; Bachelder, E. M.; Cohen, J. A.; Obermeyer, A. C.; Broaders, K. E.; Frechet, J. M. J.; Kang, E. S.; Mende, I.; Tseng, W. W.; Davidson, M. G.; Engleman, E. G. In Vivo Studies on the Effect of Co-Encapsulation of CpG DNA and Antigen in Acid-Degradable Microparticle Vaccines. *Mol. Pharmaceutics* **2009**, *6*, 1160−1169.
(39) Zwiorek, K.; Bourquin, C.; Battiany, J.; Winter, G.; Endres, S.; Hartmann, G.; Coester, C. Delivery by Cationic Gelatin Nanoparticles Strongly Increases the Immunostimulatory Effects of CpG Oligonucleotides. *Pharm. Res.* **2008**, *25*, 551−562.
(40) Wilson, K. D.; de Jong, S. D.; Tam, Y. K. Lipid-Based Delivery of CpG Oligonucleotides Enhances Immunotherapeutic Efficacy. *Adv. Drug Delivery Rev.* **2009**, *61*, 233−242.
(41) Jain, S.; Yap, W. T.; Irvine, D. J. Synthesis of Protein-Loaded Hydrogel Particles in an Aqueous Two-phase System for Coincident Antigen and CpG Oligonucleotide Delivery to Antigen-Presenting Cells. *Biomacromolecules* **2005**, *6*, 2590−2600.
(42) Fonseca, D. E.; Kline, J. N. Use of CpG Oligonucleotides in Treatment of Asthma and Allergic Disease. *Adv. Drug Delivery Rev.* **2009**, *61*, 256−262.
(43) Rattanakiat, S.; Nishikawa, M.; Funabashi, H.; Luo, D.; Takakura, Y. The Assembly of a Short Linear Natural Cytosine-Phosphate-Guanine DNA into Dendritic Structures and its Effect on Immunostimulatory Activity. *Biomaterials* **2009**, *30*, 5701−6.
(44) Bianco, A.; Hoebeke, J.; Godefroy, S.; Chaloin, O.; Pantarotto, D.; Briand, J.-P.; Muller, S.; Prato, M.; Partidos, C. D. Cationic Carbon Nanotubes Bind to CpG Oligodeoxynucleotides and Enhance Their Immunostimulatory Properties. *J. Am. Chem. Soc.* **2005**, *127*, 58−59.
(45) Wei, M.; Chen, N.; Li, J.; Yin, M.; Liang, L.; He, Y.; Song, H.; Fan, C.; Huang, Q. Polyvalent Immunostimulatory Nanoagents with Self-Assembled CpG Oligonucleotide-Conjugated Gold Nanoparticles. *Angew. Chem., Int. Ed. Engl.* **2012**, *51*, 1202−6.
(46) Li, J.; Pei, H.; Zhu, B.; Liang, L.; Wei, M.; He, Y.; Chen, N.; Li, D.; Huang, Q.; Fan, C. Self-Assembled Multivalent DNA Nanostructures for Noninvasive Intracellular Delivery of Immunostimulatory CpG Oligonucleotides. *ACS Nano* **2011**, *5*, 8783−9.
(47) Chen, N.; Wei, M.; Sun, Y.; Li, F.; Pei, H.; Li, X.; Su, S.; He, Y.; Wang, L.; Shi, J.; Fan, C.; Huang, Q. Self-Assembly of Poly-Adenine-Tailed CpG Oligonucleotide-Gold Nanoparticle Nanoconjugates with Immunostimulatory Activity. *Small* **2013**, *10*, 368−75.

(48) Wang, Z.; Ge, Z.; Zheng, X.; Chen, N.; Peng, C.; Fan, C.; Huang, Q. Polyvalent DNA-Graphene Nanosheets "Click" Conjugates. *Nanoscale* **2012**, *4*, 394−9.
(49) Shan, C.; Yang, H.; Han, D.; Zhang, Q.; Ivaska, A.; Niu, L. Water-Soluble Graphene Covalently Functionalized by Biocompatible Poly-L-Lysine. *Langmuir* **2009**, *25*, 12030−3.